Spektrum Industri
Vol. 21, No. 2, 2023, pp. 149-158
ISSN 1693-6590
http://journal3.uad.ac.id/index.php/spektrum

Analyzing Thermal Processes in Laser Welding of Multi-Component Heat-Resistant Alloy Thin-Walled Butt Joints: A Comprehensive Modeling Approach

Mykola Sokolovskyi [a], Artemii Bernatskyi [a*], Oleksandr Siora [a], Valentyna Bondarieva [a], Yurii Yurchenko [a], Nataliia Shamsutdinova [a,b], Oleksandr Danyleiko [a,b]

[a] Department of Specialized High-Voltage Technique and Laser Welding, E. O. Paton Electric Welding Institute, National Academy of Sciences of Ukraine, Kyiv, Ukraine
[b] Department of Laser Systems and Advanced Technologies, E. O. Paton Educational and Research Institute of Material Science and Welding, National Technical University of Ukraine, Kyiv, Ukraine
* Corresponding Author : bernatskyi@paton.kiev.ua

ARTICLE INFO

Article history
Received August 08, 2023
Revised September 11, 2023
Accepted October 15, 2023

Keywords
Laser welding;
Thin-walled parts;
Butt joints;
Alloys;
Multi-component heat-resistant

ABSTRACT

Niobium-based alloys are vital in high-temperature environments due to their unique chemical composition, phase structure, high density, and oxidation resistance. These alloys find extensive applications in industries such as medicine, engine manufacturing, and space technology. This study delves into the complexities of modeling laser welding processes, necessitated by the multitude of dynamic parameters specific to each surface configuration. Finite element modeling was conducted using COMSOL Multiphysics to analyze the heat transfer in butt joints between Nb-15W-5Mo-1Zr alloy plates under 400 W laser radiation power. The research employed finite element modeling to analyze heat transfer in Nb-15W-5Mo-1Zr alloy plates, considering non-uniform movement at the start and end of the welding process, Gaussian heat flux distribution along the laser spot radius, and temperature-dependent reflection coefficient. The models accounted for non-uniform movement, Gaussian heat flux distribution, and temperature-dependent reflection coefficient. The study demonstrated that thin plates of Nb-15W-5Mo-1Zr alloy can be effectively welded using specific laser processing modes, leveraging their high initial cooling rate of 1.2-1.3 s. Successful welding of Nb-15W-5Mo-1Zr alloy plates requires careful consideration of laser processing parameters. While the alloy's thermodynamic properties allow for effective welding, ensuring weld quality mandates additional production processes aimed at preventing potential part failure.

1. Introduction

Niobium-based alloys have emerged as a rapidly advancing group of heat-resistant materials, widely employed across diverse industries due to their exceptional performance in high-temperature environments (Wojcik, 1993). Their superior properties, rooted in a complex interplay of chemical composition, phase structure (Hon et al., 2003; Zhang et al., 2023), high density, and oxidation resistance at elevated temperatures (Tanaka et al., 2004; Chou et al., 1997), have facilitated their

applications in critical sectors such as medicine (Zardiackas et al., 2006; Xu et al., 2013), engine manufacturing (Tanaka et al., 2004; Stechman et al., 2000; Liu et al., 2004), and the space industry (Stechman et al., 2000; Liu et al., 2004; Diaz-Aguado et al., 2019).

The widespread use of niobium-based alloys has sparked extensive research focused on manufacturing parts from these materials. However, challenges arise from the intricate factors influencing their high-temperature performance, posing difficulties in the manufacturing process. Consequently, numerous studies have explored various manufacturing methods, encompassing thermo-mechanical processes (Vishwanadh et al., 2023), powder metallurgy (Loria, 1987), electron-beam techniques (Ali & K. Vadali, 2016; Yang et al., 2021), and laser welding (Quazi et al., 2020) (Shelyagin et al., 2021; Bernatskyi, 2021). Among these methods, laser welding has garnered particular attention.

In conventional welding processes, energy is deposited on the workpiece surface and then conducted internally through heat conduction mechanisms (Fabbro & Chouf, 2000). Laser welding, however, uniquely concentrates energy deep within a narrow cavity formed by the incident beam (Torkamany, Malek Ghaini, & Poursalehi, 2016; Torkamany, Malek Ghaini, Poursalehi, et al., 2016; Torkamany et al., 2014). This characteristic allows the concentration of exceptionally high energy within a small area, making laser technologies invaluable for welding materials with minimal thermal distortion and metallurgical damage, albeit posing a challenge in modeling these processes.

The focus of this study arises from the need to develop scientific foundations and technological methods for laser welding multicomponent heat-resistant alloys, especially for aerospace applications. Modeling the thermal processes during laser welding of thin-walled butt joints in multicomponent heat-resistant alloys became imperative. The physics of welding thin-walled metals significantly differs from that of semi-infinite bodies, necessitating a shift towards accurate modeling to understand these complexities.

Modeling these intricate processes proves highly complex, given the multitude of dynamic parameters unique to each surface configuration. To address this complexity, specific requirements and conventions were established to ensure accurate calculations. The heat exchange models devised adhere to several critical principles, including (1) consideration of boiling point, reflection coefficient, and heat of vaporization, (2) accounting for material characteristic nonlinearity in thermal field calculations, and (3) incorporation of the non-linear relationship of heat loss, a pivotal factor establishing quasi-equilibrium in the melt bath. However, to streamline the calculation process, certain simplifications were adopted such as (1) exclusion of surface deformation in solid and liquid phases, (2) omission of liquid melt movement and re-reflection of the laser beam within the melting channel, and (3) partial consideration of the creation of a melt bath in the form of a melting channel and a steam-gas channel.

The contribution of this study, these principles and conventions were rigorously applied to conduct a comprehensive theoretical calculation of thermal field dynamics during the formation of welds in Nb-15W-5Mo-1Zr steel with a thickness of 0.8 mm. Through this detailed analysis, this research aims to shed light on the intricate nuances of laser welding processes in thin-walled niobium-based alloy parts, contributing significantly to the advancement of aerospace manufacturing techniques.

2. Method

The Nb-15W-5Mo-1Zr alloy, also known as the F-48 alloy, is a heat-resistant niobium alloy used in the manufacture of parts for turbines, jet engines and nuclear reactors (Wojcik, 1993; Tanaka et al., 2004). The main working temperature of the alloy is 800-1400°C. The melting point is 2540°C. The composition of the material is shown in Table 1.

Table 1. Composition of the Nb-15W-5Mo-1Zr alloy

Element	Nb	W	Mo	Zr	C
Mass percentile (%)	Balance	14.95-15.2	4.92-5.07	0.93-0.98	~0.1

The models were made using the physical module Heat Transfer in Solids (ht) of the CAD complex COMSOL Multiphysics 5.6.0.149. This module calculates thermal processes during laser radiation according to a mathematical model based on the Stefan-Boltzmann law, namely according to equation 1.

$$\rho C_p\left(\frac{\partial T}{\partial t}+\mathbf{u}_{\text{trans}}\cdot\nabla T\right)+\nabla\cdot(\mathbf{q}+\mathbf{q}_r)=-\alpha T:\frac{dS}{dt}+Q \quad (1)$$

where: ρ - density [kg / m3]; Cp - specific heat capacity at constant stress [J / (kg*K)]; T - absolute temperature [K]; utrans - translation speed vector [m/s]; q - heat flow by conductivity [W / m2]; qr - radiation heat flow [W / m2]; α - coefficient of thermal expansion [1 / K]; S - the second Piola-Kirchhoff stress tensor [Pa]; Q - additional heat sources [W / m3].

The thermal footprint of this process (Q1) is calculated using equation 2, which takes into account the Gaussian distribution of energy.

Q1=Laser_power*(1-Rc)*1/(pi*beam_radius_x^2)*Gauss2D(x,x00) (2)

The parameters of the processing modes used in these experiments are listed in Table 2.

Table 2. Characteristics of Heat Transfer in Solids

Designation	Value	Characteristic
x0	"0 [mm]"	Pulse center on x coordinate
y0	"0 [mm]"	Pulse center on y coordinate
beam_radius_x	51 [µm]	Laser beam radius in x direction
beam_radius_y	51 [µm]	Laser beam radius in y direction
Laser_power	400 [W]	Lotal power of the laser beam
Rc	0.3	Laser beam reflecion coefficient
Width	50 [mm]	Width
Height	20 [mm]	Height
v	300 [mm/min]	Laser beam travel speed
Thickness	0.8 [mm]	Material thickness
r_spot	51 [µm]	Laser beam radius

The Gaussian distribution in the model is given by the Gauss2D equation (3) with limits, provided in table 3.

exp(-(x-x0)^2/(2*beam_radius_x^2)) (3)

Table 3. Framework of the Gaussian distribution formula

x	-2*beam_radius_x	2*beam_radius_x
x0	0	0

The graph of the obtained Gaussian distribution is shown in Fig. 1.

Spektrum Industri
Vol. 21, No. 2, 2023, pp. 149-158
ISSN 1693-6590

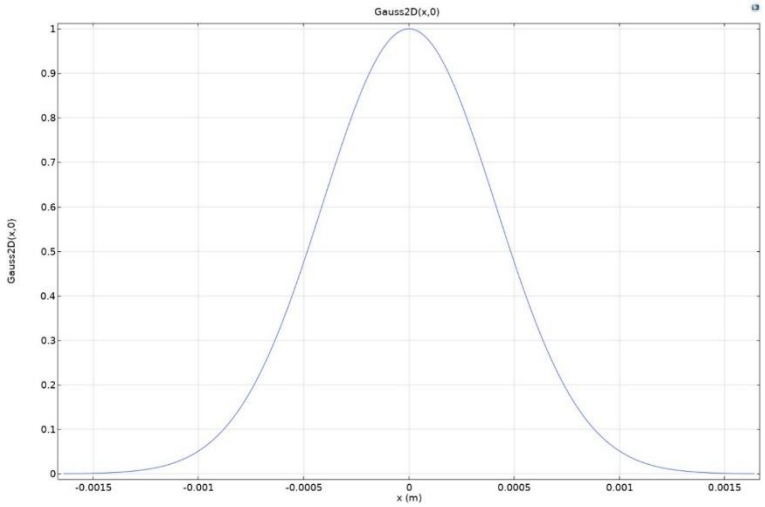

Fig 1. Graph of the Gaussian distribution of laser radiation used in the calculations.

The model itself is a two-plate body, which is modeled within constraints of Thermal Insulation and Heat Flux modules. The calculated area is two plates with dimensions of 50×20×0.8 mm. Laser radiation passes the welding line with a uniform 300 mm/min speed. Gas protection is absent. To clarify the results, the calculation mesh (Fig 2) was refined in the butt area between the two plates.

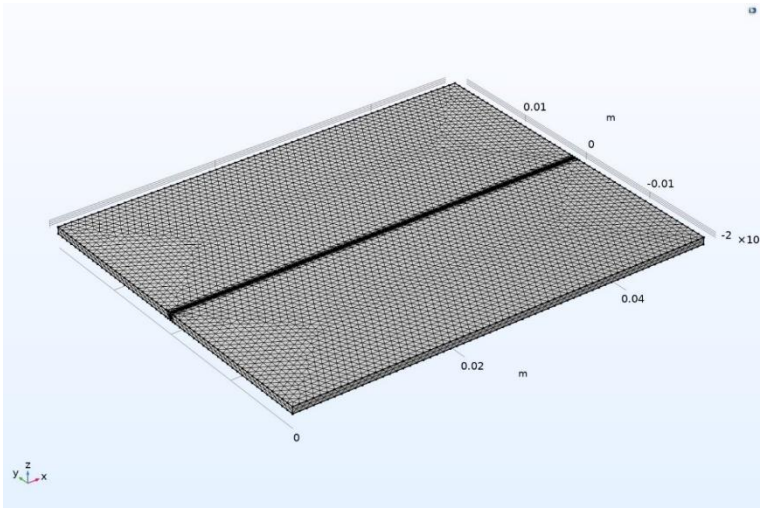

Fig 2. The geometry of the model with the calculation mesh applied to it

3. Results and Discussion

It was expected that as a result of the modelling, a thermal calculation model of the convective type with a uniform distribution of thermal energy. The Gaussian distribution of energy is observed over the entire surface plane, the temperature on the surface exceeds the melting point of the material. At the same time, it is known that the obtained 2D shapes of the melt pools will not exactly coincide with the experimental ones due to the chosen conventions in the calculation, since they do not take into account physical phenomena that strongly affect the shape of the melt pool and, as a result, the weld.

During laser processing of this alloy in a semi-infinite body, it was observed that most of the melting of the material occurs after 0.1-0.2s after the transfer of energy by laser radiation. This is

clearly visible in Fig. 3, which shows a section of the end of the calculation zone during the passage of the LV through its plane. At the same time, this alloy has a pronounced scheme of convective heat exchange, spreading thermal energy horizontally by 1.1-1.2 mm in both directions, ensuring full penetration of the plate.

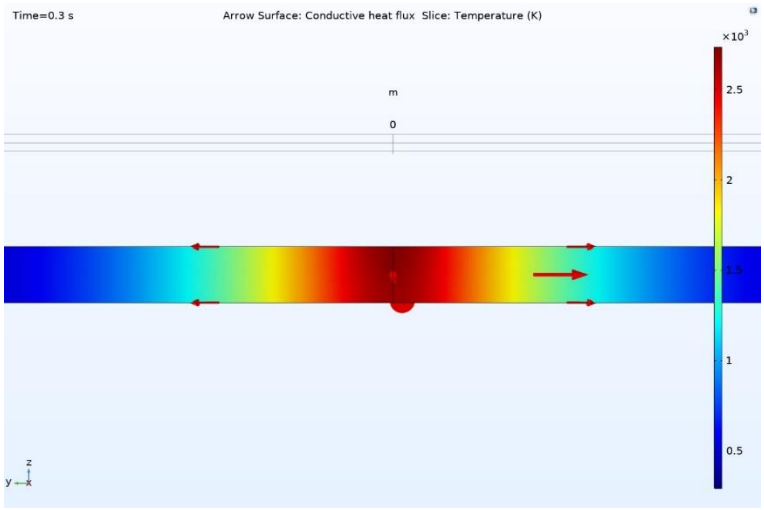

Fig. 3. Model of heat exchange in the YZ plane during laser welding of plates of the Nb-15W-5Mo-1Zr LV alloy with a power of 400 W, moment of time 0.3s (cross-section)

In this case, the temperature of the surface layers of the material reaches the material's evaporation point, emphasizing the need to use gas protection. The short length of the zone (as shown in Fig. 4), where the temperature of the material remains higher than the melting temperature (about 2-2.5 mm), indicates a high initial cooling rate of the alloy without external influences (Zhou et al., 2020; K. Liu et al., 2021). This can be explained by the physical composition of the alloy. At the same time, it is possible to notice a rather long (approximately 14.8 mm) zone where the material temperature remains higher than the temperature of the working mode of this alloy (1500-2200 oC), which indicates a rapid decrease in the cooling rate after recrystallization of the metal (Chen et al., 2017; Yadollahi et al., 2015). The homogeneity of preservation of the convective nature of the thermodynamic interaction of processes is preserved. With the selected processing modes, a complete fading of the points of the thin plates was observed 0-0.1 s after the application of laser radiation to these points.

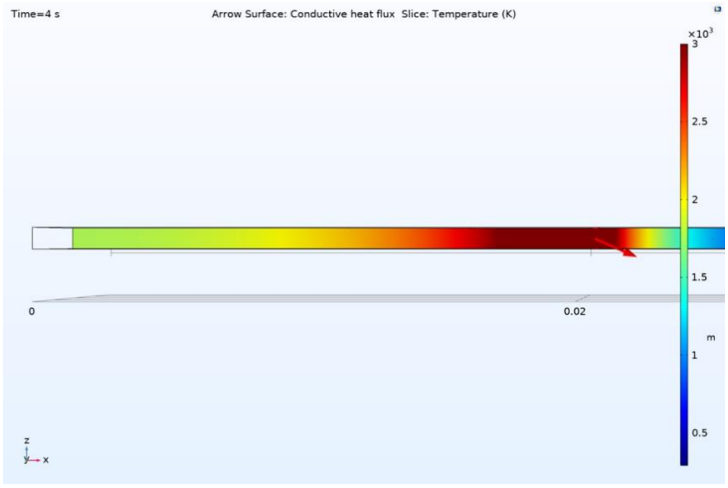

Fig 4. Scheme of heat exchange in the XZ plane during laser welding of plates of the Nb-15W-5Mo-1Zr LV alloy with a power of 400 W, moment of time 4s (cross-section)

Spektrum Industri
Vol. 21, No. 2, 2023, pp. 149-158
ISSN 1693-6590

A clearer picture in the horizontal plane, which is caused by the action of laser radiation in the Nb-15W-5Mo-1Zr alloy, is shown in Fig. 5 and Fig. 6.

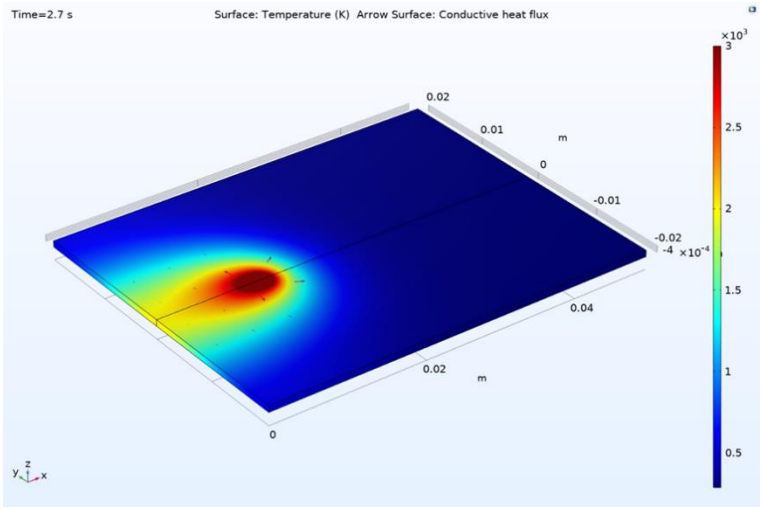

Fig 5. Top-down view of heat exchange during laser welding of plates of the Nb-15W-5Mo-1Zr LV alloy with a power of 400 W, moment of time 2.7s (upper side)

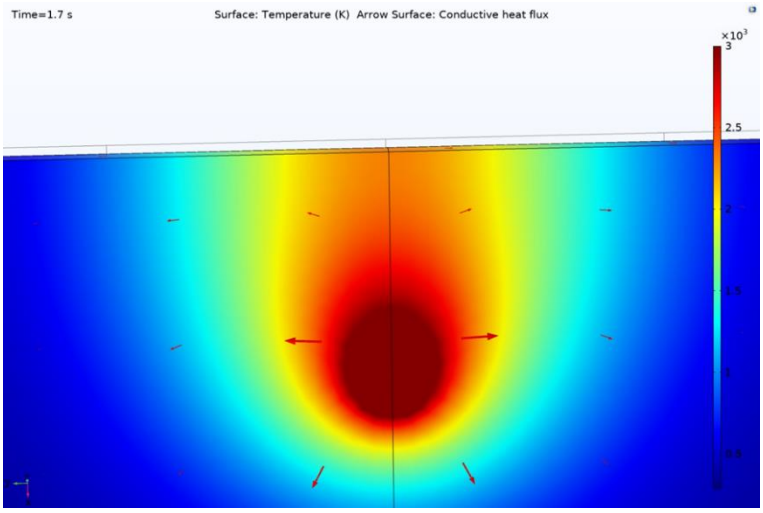

Fig 6. Top-down view of heat exchange during laser welding of plates of the Nb-15W-5Mo-1Zr LV alloy with a power of 400 W, moment of time 1.7s (lower side)

Here, it can be seen that approximately 65% of the heat exchange (the direction of which is shown by the arrows in Fig. 5 and Fig. 6) takes place directly next to the zone of direct action of the LV. At the same time, due to the small thickness of the material, the main part of the absorbed thermal energy goes to the horizontal, not the vertical plane (Seddegh et al., 2016; Yang et al., 2016). For a direct comparison of the results of calculations and data on the rate of cooling of the material, graphs of the temperature distribution in depth were formulated and given (Fig. 7 and Fig. 8).

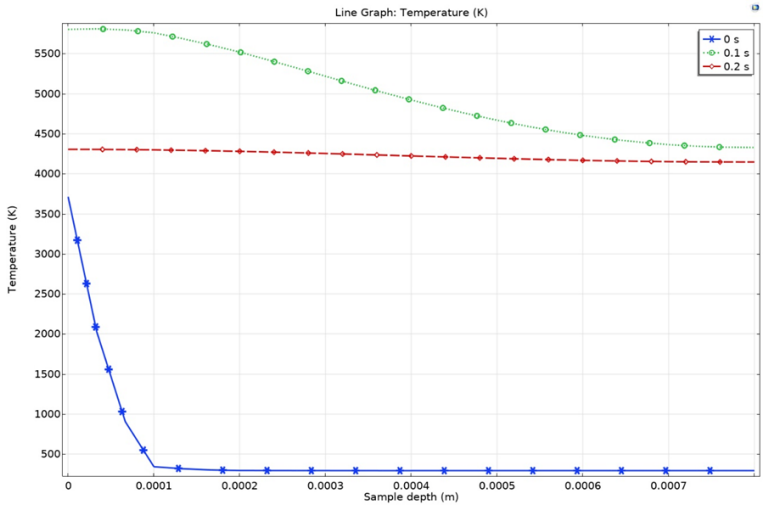

Fig 7. Graph of temperature distribution along the XZ plane during laser welding of plates of the Nb-15W-5Mo-1Zr LV alloy with a power of 400 W

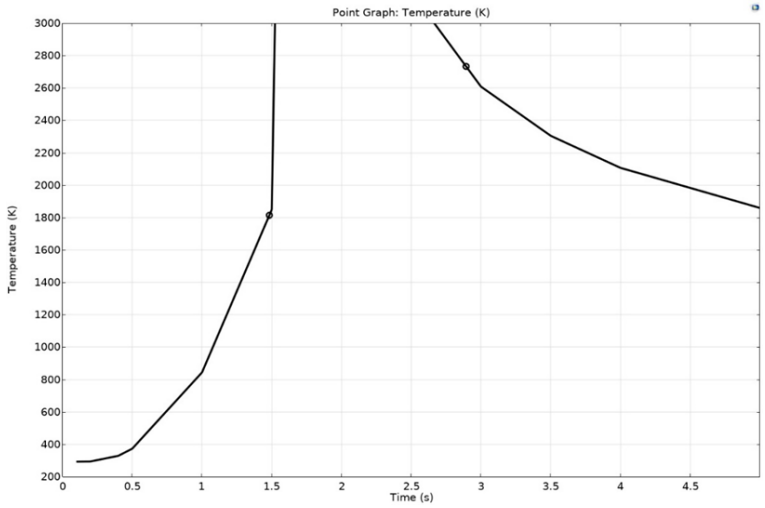

Fig 8. Graph of temperature distribution on the surface of the plate at a distance of 10 mm from the end during laser welding of plates of the Nb-15W-5Mo-1Zr LV alloy with a power of 400 W

The solidification time of the melt is 1.25-1.3 s. At the same time, the cooling rate drops sharply to ~200oC/s in 1.4-1.7 seconds after the material solidifies. After that, the cooling rate of the material decreases even more, emphasizing the need to ensure cooling (Souayfane et al., 2016). Finally, to identify differences in the dynamics of the thermal process, an analysis of the isothermal contours of the heat exchange process, shown in Fig. 9.

Spektrum Industri
Vol. 21, No. 2, 2023, pp. 149-158
ISSN 1693-6590

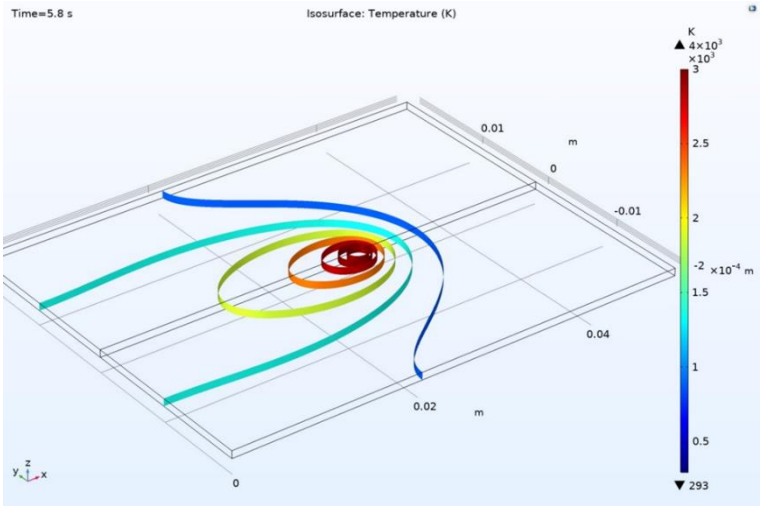

Fig 9. Isothermal contour of the instantaneous melt bath during laser welding of plates of the Nb-15W-5Mo-1Zr alloy with a power of 400 W, time 5.8 s.

When welding butt joints of thin-walled plates from this material, an elliptical melt bath with an elongation of 4-5.6 mm and a width of 2.1-2.3 mm is formed. Analysis of the thermodynamic interaction of thin plates made of the Nb-15W-5Mo-1Zr alloy showed a series of dependencies, namely (1) when calculating laser processing processes, it is important to take into account many factors, such as the thermodynamic effect on the placement of the liquid phase in the melt bath and (2) the Nb-15W-5Mo-1Zr alloy is quite difficult to process by laser processing due to its extremely heat-resistant composition, while having a higher cooling rate and a relatively uniform temperature distribution in three planes (Maruda et al., 2016).

From the results of modeling the thermodynamic interaction of this alloy during laser processing, it can be fairly confidently said that the selected processing modes make it possible to laser weld plates with a thickness of 0.8-1.2 mm without serious changes to the characteristics of laser radiation. At the same time, a high but rapidly falling cooling rate, as well as a wide melt bath, indicate the need for sufficient quality control by protecting the heat-affected zone by using complex technological methods.

4. Conclusion

Modeling of thermal processes occurring during laser welding of thin-walled butt joints of multicomponent heat-resistant alloys is an extremely complex process due to the large number of dynamic parameters that must be selected individually for each configuration of the treated surfaces. To ensure the fulfillment of the task, an analysis of thermal processes was performed and a model of butt joint of thin plates made of multi-component metals was created. As a result, a model of a welded joint with full penetration of the entire thickness of the welded plates with a wide weld seam and a heat-affected zone was obtained. Thin plates made of Nb-15W-5Mo-1Zr (F-48) alloy, due to their thermodynamic properties (such as a high initial cooling rate of 1.2-1.3 s), can be welded by selected laser processing modes. At the same time, it should be noted that the quality of the weld in this case must be ensured by a complex of auxiliary production processes aimed at preventing the possible failure of the part.

Author Contribution: All authors contributed equally to the main contributor to this paper. All authors read and approved the final paper.

Funding: This research received no external funding

Conflicts of Interest: Declare conflicts of interest or state, “The authors declare no conflict of interest.”

References

Ali, M., & K. Vadali, S. (2016). Development of Electron Beam Welding Procedure for Nb-1Zr-0.1C Alloy. *Materials Today: Proceedings*, *3*(9, Part B), 2913–2919. https://doi.org/10.1016/j.matpr.2016.09.003

Bernatskyi, A. (2021). Determination of the Influence of Laser Welding Parameters on the Weld Quality Assurance of Heat-Resistant Alloys. *International Journal for Research in Applied Science and Engineering Technology*, *9*(12), 612–615. https://doi.org/10.22214/ijraset.2021.39313

Chen, H., Gu, D., Dai, D., Ma, C., & Xia, M. (2017). Microstructure and composition homogeneity, tensile property, and underlying thermal physical mechanism of selective laser melting tool steel parts. *Materials Science and Engineering: A*, *682*, 279–289. https://doi.org/10.1016/j.msea.2016.11.047

Chou, I., Koss, D. A., Howell, P. R., & Ramani, A. S. (1997). High-temperature deformation of a mechanically alloyed niobium-yttria alloy. *Materials Science and Engineering: A*, *222*(1), 14–20. https://doi.org/10.1016/S0921-5093(96)10450-0

Diaz-Aguado, M. F., Bonnell, J. W., Bale, S. D., Rezvani, S. J., Koshmak, K., Giglia, A., Nannarone, S., & Gruntman, M. (2019). Experimental Investigation of Total Photoemission Yield from New Satellite Surface Materials. *Journal of Spacecraft and Rockets*, *56*(1), 248–258. https://doi.org/10.2514/1.A34245

Fabbro, R., & Chouf, K. (2000). Keyhole modeling during laser welding. *Journal of Applied Physics*, *87*(9), 4075–4083. https://doi.org/10.1063/1.373033

Heisterkamp, F., & Carneiro, T. (2001). Niobium, Science & Technology 2001. *Proceedings of the International Symposium Niobium*, 1109–1160.

Hon, Y.-H., Wang, J.-Y., & Pan, Y.-N. (2003). Composition/Phase Structure and Properties of Titanium-Niobium Alloys. *Materials Transactions*, *44*(11), 2384–2390. https://doi.org/10.2320/matertrans.44.2384

Liu, C., Chen, J., Han, H., Wang, Y., & Zhang, Z. (2004). A long duration and high reliability liquid apogee engine for satellites. *Acta Astronautica*, *55*(3), 401–408. https://doi.org/10.1016/j.actaastro.2004.05.030

Liu, K., Chen, P., Feng, J., Ran, C., Wang, Y., Zhou, Q., & Zhu, L. (2021). Fabrication and characterization of the Mo/cu bimetal with thick Mo layer and high interfacial strength. *International Journal of Refractory Metals and Hard Materials*, *94*, 105383. https://doi.org/10.1016/j.ijrmhm.2020.105383

Loria, E. A. (1987). Niobium-Base Superalloys via Powder Metallurgy Technology. *JOM*, *39*(7), 22–26. https://doi.org/10.1007/BF03258035

Maruda, R. W., Krolczyk, G. M., Nieslony, P., Wojciechowski, S., Michalski, M., & Legutko, S. (2016). The influence of the cooling conditions on the cutting tool wear and the chip formation mechanism. *Journal of Manufacturing Processes*, *24*, 107–115. https://doi.org/10.1016/j.jmapro.2016.08.006

Quazi, M. M., Ishak, M., Fazal, M. A., Arslan, A., Rubaiee, S., Qaban, A., Aiman, M. H., Sultan, T., Ali, M. M., & Manladan, S. M. (2020). Current research and development status of dissimilar materials laser welding of titanium and its alloys. *Optics & Laser Technology*, *126*, 106090. https://doi.org/10.1016/j.optlastec.2020.106090

Seddegh, S., Wang, X., & Henderson, A. D. (2016). A comparative study of thermal behaviour of a horizontal and vertical shell-and-tube energy storage using phase change materials. *Applied Thermal Engineering*, *93*, 348–358. https://doi.org/10.1016/j.applthermaleng.2015.09.107

Shelyagin, V. D., E.O. Paton Electric Welding Institute, NASU, Bernatskyi, A. V., E.O. Paton Electric Welding Institute, NASU, Siora, O. V., E.O. Paton Electric Welding Institute, NASU, Bondarieva, V. I., E.O. Paton Electric Welding Institute, NASU, Brodnikovsky, M. P., & I.M. Frantsevich Institute of Problems of Materials Science, NASU. (2021). Structure of laser welded joints of multicomponent high-entropy alloy of Nb-Cr-Ti-Al-Zr system. *Avtomatičeskaâ Svarka (Kiev)*, *2021*(6), 29–34. https://doi.org/10.37434/as2021.06.04

Souayfane, F., Fardoun, F., & Biwole, P.-H. (2016). Phase change materials (PCM) for cooling applications in buildings: A review. *Energy and Buildings*, *129*, 396–431. https://doi.org/10.1016/j.enbuild.2016.04.006

Stechman, C., Woll, P., Fuller, R., & Colette, A. (2000). A high performance liquid rocket engine for satellite main propulsion. In *36th AIAA/ASME/SAE/ASEE Joint Propulsion Conference and Exhibit*. American Institute of Aeronautics and Astronautics. https://doi.org/10.2514/6.2000-3161

Tanaka, R., Kasama, A., Fujikura, M., Iwanaga, I., Tanaka, H., & Matsumura, Y. (2004). Newly developed niobium-based superalloys for elevated temperature application. *Proceedings of the International Symposium on Niobium for High Temperature Applications*, 89–98.

Torkamany, M. J., Malek Ghaini, F., & Poursalehi, R. (2014). Dissimilar pulsed Nd:YAG laser welding of pure niobium to Ti–6Al–4V. *Materials & Design*, *53*, 915–920. https://doi.org/10.1016/j.matdes.2013.07.094

Torkamany, M. J., Malek Ghaini, F., & Poursalehi, R. (2016). An insight to the mechanism of weld penetration in dissimilar pulsed laser welding of niobium and Ti–6Al–4V. *Optics & Laser Technology*, *79*, 100–107. https://doi.org/10.1016/j.optlastec.2015.11.005

Torkamany, M. J., Malek Ghaini, F., Poursalehi, R., & Kaplan, A. F. H. (2016). Combination of laser keyhole and conduction welding: Dissimilar laser welding of niobium and Ti-6Al-4V. *Optics and Lasers in Engineering*, *79*, 9–15. https://doi.org/10.1016/j.optlaseng.2015.11.001

Vishwanadh, B., Kumar, N. N., Samyuktha, G., Kaushik, V., & Tewari, R. (2023). Development of a new thermo-mechanical processing route for Nb-5Mo-1Zr-0.1C (wt%) alloy. *Journal of Alloys and Compounds*, *942*, 168860. https://doi.org/10.1016/j.jallcom.2023.168860

Wojcik, C. C. (1993). Processing, Properties and Applications of High-Temperature Niobium Alloys. *MRS Online Proceedings Library*, *322*(1), 519–530. https://doi.org/10.1557/PROC-322-519

Xu, J., Weng, X.-J., Wang, X., Huang, J.-Z., Zhang, C., Muhammad, H., Ma, X., & Liao, Q.-D. (2013). Potential Use of Porous Titanium–Niobium Alloy in Orthopedic Implants: Preparation and Experimental Study of Its Biocompatibility In Vitro. *PLOS ONE*, *8*(11), e79289. https://doi.org/10.1371/journal.pone.0079289

Yadollahi, A., Shamsaei, N., Thompson, S. M., & Seely, D. W. (2015). Effects of process time interval and heat treatment on the mechanical and microstructural properties of direct laser deposited 316L stainless steel. *Materials Science and Engineering: A*, *644*, 171–183. https://doi.org/10.1016/j.msea.2015.07.056

Yang, J., Huang, Y., Liu, B., Guo, C., & Sun, J. (2021). Precipitation behavior in a Nb-5W-2Mo-1Zr niobium alloy fabricated by electron beam selective melting. *Materials Characterization*, *174*, 111019. https://doi.org/10.1016/j.matchar.2021.111019

Yang, J., Yang, L., Xu, C., & Du, X. (2016). Experimental study on enhancement of thermal energy storage with phase-change material. *Applied Energy*, *169*, 164–176. https://doi.org/10.1016/j.apenergy.2016.02.028

Zardiackas, L., Freese, H., & Kraay, M. (Eds.). (2006). *Titanium, Niobium, Zirconium, and Tantalum for Medical and Surgical Applications*. ASTM International. https://doi.org/10.1520/STP1471-EB

Zhang, Y., Wei, Q., Xie, P., & Xu, X. (2023). An ultrastrong niobium alloy enabled by refractory carbide and eutectic structure. *Materials Research Letters*, *11*(3), 169–178. https://doi.org/10.1080/21663831.2022.2133977

Zhou, J., Wang, Q., Hui, X., Zeng, Q., Xiong, Y., Yin, K., Sun, B., Sun, L., Stoica, M., Wang, W., & Shen, B. (2020). A novel FeNi-based bulk metallic glass with high notch toughness over 70 MPa m1/2 combined with excellent soft magnetic properties. *Materials & Design*, *191*, 108597. https://doi.org/10.1016/j.matdes.2020.108597